Dynamics of Impact Cratering in Shallow Sand Layers

J. F. Boudet, Y. Amarouchene, and H. Kellay

Centre de Physique Moléculaire Optique et Hertzienne (UMR 5798), U. Bordeaux 1, 351 cours de la Libération, 33405 Talence France

(Received 25 January 2006; published 19 April 2006)

When a solid sphere impacts a shallow layer of sand deposited on a solid surface, a crater can be obtained. The dynamics of the opening of the crater can be followed accurately. During this opening, the radius of the crater can be conveniently modeled by an exponential saturation with a well-defined time constant. The crater then closes up partially once the opening phase is over as the sand avalanches down the slope of the crater. We here present a detailed study of the full dynamics of the crater formation as well as the dynamics of the corrola formed during this process. A simple model accounts for most of our observations.

DOI: 10.1103/PhysRevLett.96.158001 PACS numbers: 45.70.Ht, 45.70.Mg, 45.70.Qj

The formation of a crater following an impact may at first sight seem complex and probably out of reach for a detailed understanding. Craters are, however, ubiquitous on the surface of the Moon and on the surface of Earth following impact by meteorites. While several crater properties are known [1–4], one may ask whether model experiments can be carried out to understand their formation. However, naturally occurring craters have their origin in hypervelocity impacts, and are therefore very difficult to obtain in the laboratory. These hypervelocity impacts give rise to very different initial properties than low velocity impacts which are readily studied in a laboratory setting. Still, one may hope that the final stages of the excavation of the crater may have some analogies with the final stages of low velocity impacts. Recently it was suggested that the use of granular materials in model experiments may shed some light on the complicated processes involved in crater formation for low velocity impacts on deep sand layers [5–9].

In this study, we have chosen a different strategy. Instead of using deep layers of sand, we study crater formation in shallow layers. Indeed, by studying shallow layers, we are able through direct visualization to characterize the dynamics of opening of the crater. We have observed that the crater first opens then closes partially. The results show that the opening dynamics is conveniently modeled by an exponential saturation, that the partial closing can be understood through the dynamics of avalanching, and that the disturbance caused by impact has a well-defined propagation velocity. The shape of the corolla caused by the impact and which is the result of ejected sand can also be understood using simple considerations. Many features observed here for low velocity impacts may have some analogies with the later stages of crater formation in geophysical settings [4].

The experiments use glass beads of different diameters d (ranging from 65 to 500 μm) deposited as loosely packed layers of thickness e (ranging from 0.1 to 1 cm) on a smooth glass plate. The impacting objects were steel balls of different diameters $2R$ (ranging from 0.2 to 1.4 cm). The layers studied had thicknesses e smaller than the radius of the steel balls R. The steel balls were released from different heights H and the ensuing impact was filmed with a fast video camera (working at 1000 to 2000 frames/second). The images were taken either from the side to visualize the ejected sand forming the corolla or from below the glass plate to visualize the circular hole formed after impact. To illustrate our observations, we show in Fig. 1 typical images of the corolla and the crater opening. The upper images on this figure show a sequence of images following the impact of a steel ball of 1 cm in diameter on a layer 0.4 cm thick composed of glass beads of 300 μm in diameter. The three images are 3 ms apart and one can see the steel ball, which has already collided with the surface and has bounced back, slightly rising as time elapses. The corolla starts out with a small diameter and small inclination angle. At a later time (6 ms later) the corolla is basically vertical with a larger diameter. In the bottom sequence of images, the layer appears white due to the scattering by the sand layer while the hole or bottom of the crater appears black due to the absence of the sand. The diameter of the hole increases rapidly with time, reaches a maximal value, then decreases to a final value at long times. These are our two main observations: the formation

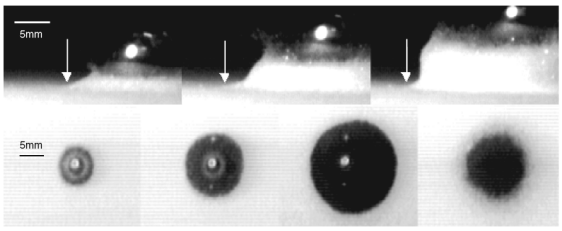

FIG. 1. Impact of a steel ball of 1 cm diameter on a 0.4 cm layer of glass beads of 300 μm in diameter. Top: sequence of images of the corolla produced by the impact; the images are 3 ms apart. Bottom: sequence of images of the produced crater, as visualized from below, at impact, 3 ms, and 15 ms after impact, and at a later time when the hole has closed up partially. The arrows point to the position of the shear disturbance as discussed in the text.

of the corolla and the opening of the crater. In what follows we analyze these two observations quantitatively.

One of the main results of this study is displayed in Fig. 2. The dynamics of the opening of the bottom of the crater, as shown in Fig. 1, is reported for a full sequence. The radius of the bottom of the crater $r(t)$ starts out increasing rapidly versus time, reaches a maximal value as the shallow maximum of the curve shows at around 20 ms, and decreases slowly afterwards to reach a final value 120 ms after the impact. The fast opening at short times is shown in the inset of Fig. 2 along with a fit to an exponential saturation of the form $r(t) = r_{\max}[1 - \exp(-t/\tau)]$. This law, which is used for convenience, gives the characteristic time τ associated with the opening process. This time is of order a few milliseconds.

The partial closing dynamics occurs at later times and has a characteristic time much longer than the opening dynamics. The closing is governed by avalanching of the beads: the opening generates a sand front which, as the radius of the crater reaches its maximal value, has a higher angle than the repose angle of the sand layer θ_r (which is around 27°). In order to understand this partial closing of the crater, we have used a theory proposed by Boutreux and de Gennes [10] for the collapse of a step of granular material. Such a step, if prepared initially with a high slope, would collapse due to avalanching grains. The theory models the dynamics of this collapse and predicts a value smaller than the angle of repose for the final state. In particular, this theory proposes that the length of the step s (see schematic in Fig. 3 for a definition) increases with time and obeys $\frac{1}{\Gamma h_0}\frac{ds}{dt} = \ln(\frac{s}{h_0}) - \theta_r \frac{s}{h_0} - k$. Here Γ is a characteristic frequency given by $\sqrt{g/d}$ where g is the gravity constant, h_0 is the step height, and k is a constant. In the experiments reported here, the variation of the diameter of the hole in the closing phase is directly related to the variation of the length of the step. In our case, $\frac{ds}{dt} = -2\frac{dr}{dt}$. Since $r(t)$ is known from the measurements in the closing phase, the variation of the step length is known as well. By integrating the equation given by Boutreux and de Gennes one can then compare theory and experiment directly. For this comparison we need to determine the initial and the final step lengths s_i and s_f. The difference $s_f - s_i$ is given by $2(r_{\max} - r_{\text{final}})$. In addition to this, the two step lengths are related to each other by the relation given above since $\frac{ds}{dt}$ is zero at the initial and final stages. The comparison between theory and experiment is shown in Fig. 3. The characteristic frequency Γ was fixed to its value given above, the repose angle is known from separate measurements, and the initial thickness is given by the layer thickness e. This figure shows that the agreement between the model predictions and the experimental results is very good. Different size grains have been used. We have also checked this model for different layer heights for which it works well for small heights but not for large heights. For large heights, and because of the circular geometry of the step used here, the two-dimensional model considered is no longer valid and the step length increases more rapidly than predicted. The good agreement observed brings forth the relevance of the characteristic frequency used so far without solid justification. As we will see below, this frequency turns out to play an important role in the dynamics of the crater formation and collapse. The model of Boutreux and de Gennes has been tested in recent experiments [11] with partial success. The parameters needed for the comparison were not in agreement with those expected from the model, and, in particular, the final slope of the step turned out to be close to the angle of repose and usually higher instead of being smaller. In our case, the final angle was systematically smaller than the

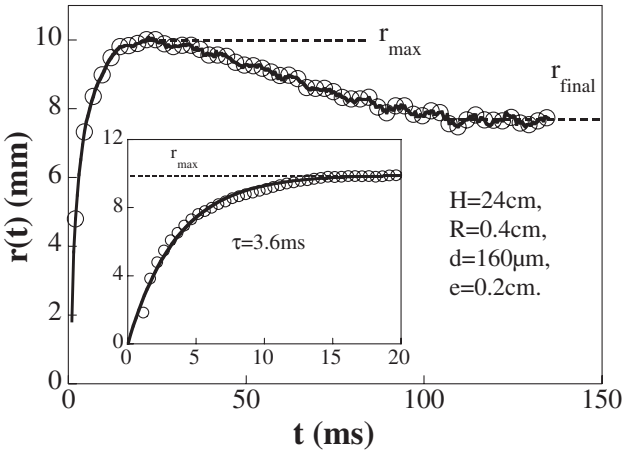

FIG. 2. The dynamics of opening of the crater: the radius of the crater vs time. Note that the crater first opens then closes partially. Inset: the initial stages of the opening of the crater; the solid line is a fit to an exponential saturation.

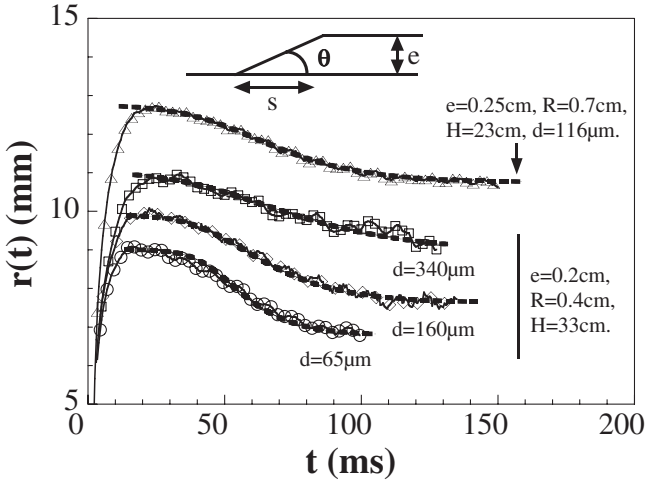

FIG. 3. The opening and closing dynamics of craters obtained under different conditions. The dashed lines are fits to the theory of Boutreux and de Gennes. The upper schematic shows a step and a definition of its length.

angle of repose as we checked through inspection of the final crater. The discrepancy observed in previous experiments may probably have different sources but let us just state that in our experiments, the layer of rolling species is probably thin, the collapse is devoid of boundary effects, and the initial angle is small.

Now, can we understand the initial stages of the opening of the craters and their relation to the dynamics of the corolla. As mentioned above and shown in Fig. 2, $r(t)$ increases according to a well defined exponential law with a well-defined characteristic time scale which is found close to the characteristic frequency Γ. The product $\Gamma\tau$ comes out to be close to 1 with a scatter of 25% from different realizations with different grains diameters and different layer heights. While the dependence versus the particle diameter is taken into account in the characteristic frequency (i.e., τ varies very roughly as $\sqrt{d}$), the dependence versus the thickness of the layer e is small with a tendency for τ to increase very slightly as e increases (τ changes by a factor 2 as e changes by a factor 5). No dependence versus H or R was noted. From the exponential law, one can deduce an initial speed for the opening given by $r_{\max}/\tau$. This speed turns out to be directly related to the speed of the impacting ball through the simple relation $r_{\max}/\tau \sim VR_e/3e$. Here V is the velocity of the impacting ball, e is the thickness of the layer, and R_e is the radius of the cross section of the ball at a height e as indicated in the schematic of Fig. 4. The initial speed is fixed by the velocity and the geometry of the ball as well as the thickness of the layer.

The initial stages of the opening of the crater are associated with the ejection of grains in the form of a corolla as seen in Fig. 1. Figure 4 shows the evolution of the shape of this corolla which starts out with a small angle with respect to the horizontal surface. This angle increases with time as the diameter of the crater increases. Since this corolla is the result of ejected grains from the layer of sand following impact, one can therefore extract the velocity of ejection from its time evolution at short times. To be more precise, we extract the position of the corolla versus time from Fig. 4 along the inclined lines (with an angle θ with respect to the horizontal surface) shown by the dashed lines in this figure. The position thus extracted varies linearly with time and a constant velocity is found along each dashed line in Fig. 4. Actually, we have chosen the inclination to be parallel to the line joining the summits of the corolla at different times. This choice of inclination is the only one giving a constant velocity along the dashed lines. One can then extract this velocity for different positions x_θ along the perpendicular to the line joining the summits (i.e., the distance between the dashed lines and the line joining the summits). The variation of this velocity with the distance x_θ is plotted in Fig. 5. While the velocity near the summit of the corolla turns out to plateau at about 1 m/s in this example, it decreases linearly with x_θ. This observation can be viewed in a simple way. As the ball impacts the layer, it pushes the grains away from the center with high velocities and they end up being ejected to form the corolla. Since the velocities extracted from the dynamics of the corolla are directly related to the ejection velocity of the grains from the layer, the velocity in the layer can then be obtained. From the linear dependence of the velocity versus x_θ, a shear rate in the layer can then be extracted. This shear rate turns out to be very close to the characteristic frequency Γ as shown in Fig. 5. This has been checked for different values of Γ by varying the diameter of the grains between 100 and 500 μm. As the schematic of Fig. 4 indicates, the grains in the layer are therefore subject to a shear rate given by Γ. Other situations have been noted to give a shear rate proportional to Γ such as the collapse of a granular step [11] or of a granular column [12].

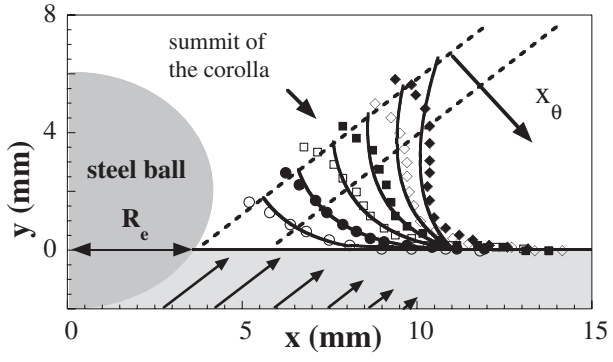

FIG. 4. The shape of the corolla produced by an impact: $R = 0.4$ cm, $H = 35$ cm, $d = 116$ μm, $e = 0.2$ cm. The solid lines are fits using the expressions in the text. The sand layer is indicated as a shaded area at the bottom. The arrows represent the velocity field produced by the impact of the ball.

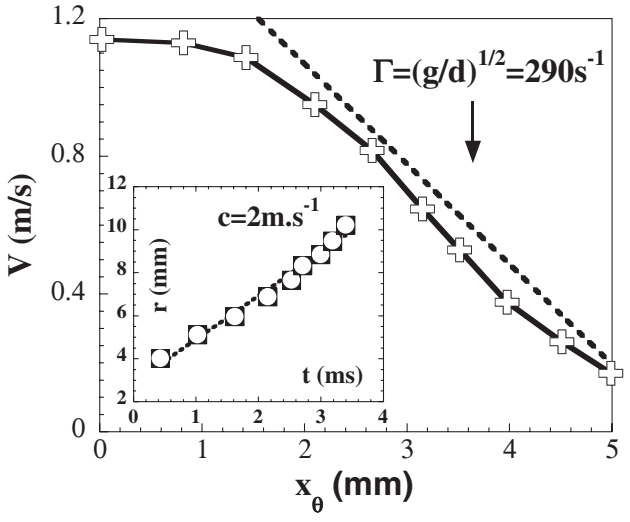

FIG. 5. The velocity profile obtained by analyzing the trajectories of different points of the corolla along inclined lines vs the distance along the perpendicular direction. Inset: position of the initial disturbance vs time giving its velocity of propagation. The parameters are the same as for Fig. 4.

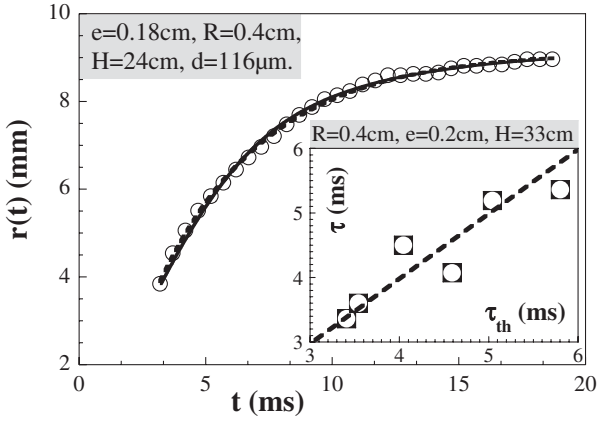

FIG. 6. The radius of the crater vs time along with a fit (dashed line) to the expression given in the text. The solid line is a fit to an exponential saturation. The inset shows the measured characteristic opening time vs the predicted one.

Another interesting observation comes from studying how the disturbance propagates right after impact. Indeed and as Fig. 1 shows, the sand layer is disturbed at its base right after the impact. By measuring the position of the disturbance (as noted by the arrows in Fig. 1) versus time, we find a characteristic horizontal velocity $c \sim 2$ m/s as shown in the inset to Fig. 5. This velocity is most probably related to the velocity of propagation of a shear disturbance in the granular material. The falling ball first generates a constant initial velocity in the layer near the impact, and this disturbance travels horizontally at the measured speed ending up establishing a constant shear rate in the layer. We did not find any systematic trend in the variation of this velocity with the grain diameter.

These observations can be used to understand both the shape of the corolla, its time evolution, and the opening dynamics of the crater. The shape of the corolla can be obtained by assuming that the grains are being ejected from the sand layer at an angle θ, subject to a velocity profile characterized by a shear rate given by Γ, and that they are ejected with a delay time given by the velocity of the initial disturbance c. This shape is given by the following expression: $x(t) = [V_0 - \Gamma r \sin(\theta)]\cos(\theta)(t - r/c) + r$ and $y(t) = [V_0 - \Gamma r \sin(\theta)]\sin(\theta)(t - r/c)$. Here V_0 is an initial velocity corresponding to the plateau value in Fig. 5, and r is the distance from the impact point. The shape of the corolla can be understood using this simple model represented by the solid lines in Fig. 4. Now, we can also relate the ejection of the sand to the variation of the radius of the hole in the opening phase. This radius corresponds to the full ejection of the sand at that position, i.e., when the sand layer rises up to a vertical position h so it is not visualized by our technique. The radius of the hole is then found from the intersection of the profiles of the corolla with a line at height h. The model predicts that the radius of the bottom of the crater obeys the following relation: $t = r(t)/c + h/[\sin(\theta)V_0(1 - r(t)\Gamma \sin(\theta)/V_0)]$. The shape obtained from inverting this relation is superimposed on the experimental curve in Fig. 6 along with an exponential saturation. The best fit gives a value of about 0.1 cm for h. The model fits the data very well giving an analytic functional shape for the opening dynamics. This shape turns out to be well approximated by the exponential saturation used above. The predicted characteristic time turns out to be $\tau_{\text{th}} = \frac{V_0}{c\Gamma \sin(\theta)} + \frac{e/2}{\sin(\theta)V_0}$, in very good agreement with our results for τ as shown in the inset to Fig. 6.

This study shows that the formation of a crater in a shallow sand layer follows simple phenomenological relations. The opening is well approximated by an exponential saturation. The final crater size is affected by avalanches and a model introduced earlier for the relaxation of a step of granular material is found to work remarkably well. The opening of the crater and the ensuing corolla can be modeled as a result of ejected sand subject to a simple shear flow and a delay time fixed by the propagation velocity of a shear disturbance in a granular material.

[1] H. J. Melosh, *Impact Cratering: A Geologic Process* (Oxford University Press, New York, 1989).
[2] H. J. Melosh and B. A. Ivanov, Annu. Rev. Earth Planet. Sci. **27**, 385 (1999).
[3] K. A. Holsapple, Annu. Rev. Earth Planet. Sci. **21**, 333 (1993).
[4] K. R. Housen and K. A. Holsapple, Icarus **163**, 102 (2003).
[5] J. C. Amato and R. E. Williams, Am. J. Phys. **66**, 141 (1998).
[6] A. M. Walsh, K. E. Holloway, P. Habdas, and J. R. deBruyn, Phys. Rev. Lett. **91**, 104301 (2003).
[7] J. S. Uehara, M. A. Ambroso, R. P. Ojha, and D. J. Durian, Phys. Rev. Lett. **90**, 194301 (2003); K. A. Newhall and D. J. Durian, Phys. Rev. E **68**, 060301(R) (2003).
[8] X. J. Zheng, Z. T. Wang, and Z. G. Qiu, Eur. Phys. J. E **13**, 321 (2004).
[9] S. T. Thoroddsen and A. Q. Shen, Phys. Fluids **13**, 4 (2001).
[10] T. Boutreux and P. G. de Gennes, C. R. Acad. Sci. Paris Serie IIb **325**, 85 (1997).
[11] S. Siavoshi and A. Kudrolli, Phys. Rev. E **71**, 051302 (2005).
[12] E. Lajeunesse, J. B. Monnier, and G. M. Homsy, Phys. Fluids **17**, 103302 (2005).